First Experimental Results with the ITER-Relevant Lower Hybrid Current Drive Launcher in Tore Supra

A. Ekedahl 1), L. Delpech 1), M. Goniche 1), D. Guilhem 1), J. Hillairet 1), M. Preynas 1), P.K. Sharma 2), J. Achard 1), Y.S. Bae 3), X. Bai 4), C. Balorin 1), Y. Baranov 5), V. Basiuk 1), A. Bécoulet 1), J. Belo 6), G. Berger-By 1), S. Brémond 1), C. Castaldo 7), S. Ceccuzzi 7), R. Cesario 7), E. Corbel 1), X. Courtois 1), J. Decker 1), E. Delmas 8), X. Ding 4), D. Douai 1), C. Goletto 1), J.P. Gunn 1), P. Hertout 1), G.T. Hoang 1), F. Imbeaux 1), K. Kirov 5), X. Litaudon 1), R. Magne 1), J. Mailloux 5), D. Mazon 1), F. Mirizzi 7), P. Mollard 1), P. Moreau 1), T. Oosako 1), V. Petrzilka 9), Y. Peysson 1), S. Poli 1), M. Prou 1), F. Saint-Laurent 1), F. Samaille 1), B. Saoutic 1)

1) CEA, IRFM, 13108 Saint Paul-lez-Durance, France.
2) Permanent address: Institute for Plasma Research, Bhat, Gandhinagar, Gujarat, India.
3) National Fusion Research Institute, Daejeon, South Korea.
4) Southwestern Institute of Physics, Chengdu, P.R. China.
5) Euratom/CCFE Fusion Association, Culham Science Centre, Abingdon, OX14 3DB, UK.
6) Associaçao Euratom-IST, Centro de Fusao Nuclear 1049-001 Lisboa, Portugal.
7) Associazione Euratom-ENEA sulla Fusione, CR Frascati, Roma, Italy.
8) Present address: ITER Organization, 13067 Saint Paul-lez-Durance, France.
9) Association Euratom-IPP.CR, Za Slovankou 3, 182 21 Praha 8, Czech Republic.

E-mail contact of main author: **annika.ekedahl@cea.fr**

Abstract. The ITER-relevant Lower Hybrid Current Drive (LHCD) launcher, based on the Passive Active Multijunction (PAM) concept, was brought into operation on the Tore Supra tokamak in autumn 2009. The PAM launcher concept was designed in view of ITER to allow efficient cooling of the waveguides, as required for long pulse operation. In addition, it offers low power reflection close to the cut-off density, which is an attractive feature for ITER, where the large distance between the plasma and the wall may bring the density in front of the launcher to low values. The experiments with the PAM on Tore Supra have shown extremely encouraging results in terms of reflected power level and power handling. Power reflection coefficient < 2% is obtained at low density in front of the launcher, i.e. close to the cut-off density, and very good agreement between the experimental results and the coupling code prediction is obtained. Long pulse operation at ITER-relevant power density has been demonstrated. The maximum power and energy reached so far is 2.7MW during 78s, corresponding to a power density of 25MW/m^2, i.e. its design value at f = 3.7GHz. In addition, 2.7MW has been coupled at a plasma-launcher distance of 10cm, with a power reflection coefficient < 2%. Finally, full non-inductive discharges of 50s have been sustained with the PAM.

1. Introduction

Lower Hybrid Current Drive (LHCD) is a well-proven method of non-inductive current drive in tokamaks and has successfully been used for current drive, volt-seconds saving and current profile shaping [1, 2] since its start in the early 1980s [3, 4]. Lower hybrid waves have the property of damping efficiently at high parallel phase velocity ($v_{//}$) relative to the electron thermal speed [5], which makes them suitable for driving a current far off-axis, where the electron temperature is lower. LHCD is therefore considered a candidate for providing far-off axis current drive in ITER, which will be required to sustain the steady-state scenario [6, 7]. One of the challenges of an LHCD system in ITER is the development of a launcher that can withstand the heat load environment in ITER under long pulses. At present, the foreseen design is based on the Passive Active Multijunction (PAM) concept, originally proposed in [8], and further detailed in the conceptual design of an LHCD system for ITER [9, 10]. The

first experimental test of a PAM module was carried out in the FTU tokamak [11, 12]. Those experiments clearly demonstrated the possibility to operate at high power density, albeit in short pulses (< 1s). Following this, a PAM launcher was designed and constructed for Tore Supra [13, 14] within the framework of the Tore Supra CIMES project [15]. The Tore Supra PAM launcher is designed to inject 2.7MW for 1000s, which corresponds to a power density of 25MW/m^2 at f = 3.7GHz and which is equivalent to the design value of 33MW/m^2 at f = 5GHz, foreseen for an LHCD system in ITER [10]. This paper will present the first experimental results obtained with this new ITER-relevant PAM launcher in Tore Supra.

2. Brief description of the PAM launcher

The Passive Active Multijunction (PAM) launcher in Tore Supra (Fig. 1) consists of 16 PAM modules, mounted in two rows and eight columns. Each PAM module itself has three waveguide rows, each with two active and two passive waveguides (Fig. 2), the passive waveguides having a depth of a quarter wavelength [9, 10]. The dimensions of the active waveguides are 14.65mm × 76mm, resulting in an active area of the launcher front equal to 0.11m^2. The PAM design allows mechanical strength to withstand disruptions and enables to put cooling channels close to the launcher front. The Tore Supra PAM launcher is actively cooled in order to be able to operate in pulse lengths of up to 1000s, once the upgraded generator capability becomes available [16, 17]. For the first experiments, the launcher was fed by eight old generation klystrons, each with a power capability of ~400kW, resulting in a total power capability of ~3MW injected to the plasma. Furthermore, the PAM design offers low reflected power level when the density in front of the launcher is low, i.e. close to the cut-off density (n_{co} = 1.7×10^{17}m^{-3} at f = 3.7GHz). This is a very attractive feature in view of ITER, where the large distance between the plasma and the wall may bring the density in front of the launcher to low values.

The main goals of the first experimental campaign with the PAM in Tore Supra were to: i) compare the power reflection coefficient on the PAM launcher against the coupling code predictions, ii) demonstrate reliable power coupling during edge perturbations mimicking ELMs and iii) achieve ITER-relevant power density, i.e. 25MW/m^2 at f = 3.7GHz, in pulse lengths exceeding several seconds.

FIG. 1. Tore Supra PAM launcher (front view).

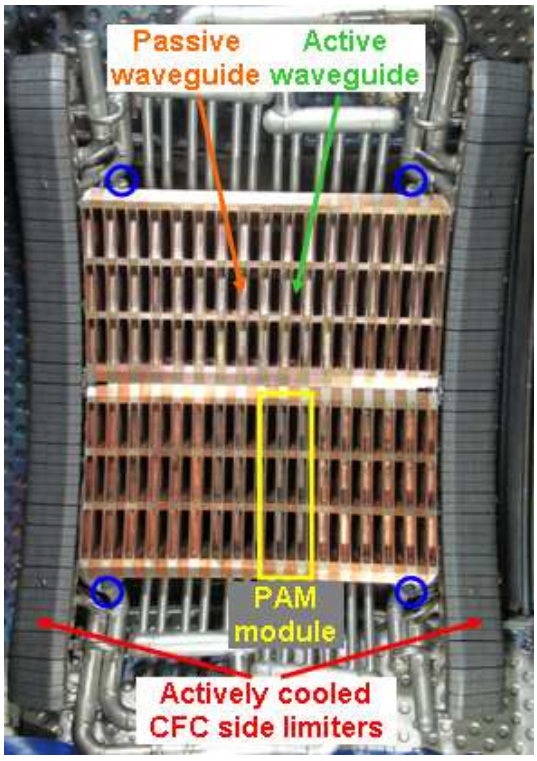

FIG. 2. The PAM launcher after installation in Tore Supra.

3. Coupling characteristics

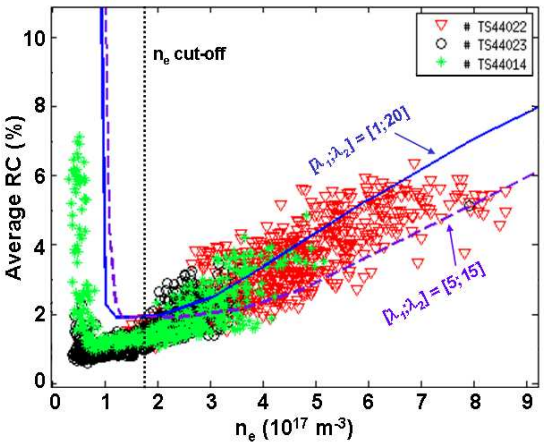

FIG. 3. Average reflection coefficient (RC) on the PAM launcher versus electron density at the launcher mouth.

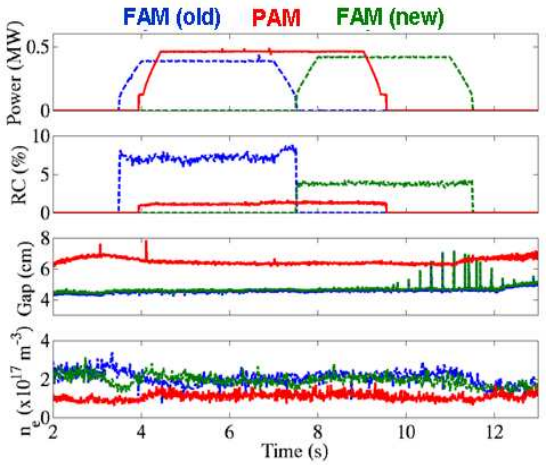

FIG. 4. Comparison of reflection coefficient on the PAM and on the two FAM launchers, used in Tore Supra.

The power reflection coefficient on the PAM launcher was studied in dedicated coupling experiments carried out at low power (200kW, i.e. ~2MW/m^2) in order to avoid possible non-linear effects that can occur at high power [18]. The density at the launcher mouth was varied from 0.5×10^{17}m^{-3} to 8×10^{17}m^{-3} by varying the position of the last closed flux surface (LCFS) during the pulse. The electron density at the launcher front was deduced from fixed Langmuir probes, mounted on the launcher. Fig. 3 shows the measured reflection coefficient (RC), averaged over the 16 modules, versus the electron density at the launcher mouth. The phasing between active waveguides was 180°, giving peak parallel refractive index $n_{//}$ = 1.72. Low reflection coefficient (RC < 2%) is obtained in the vicinity of the cut-off density. The two lines in Fig. 3 correspond to calculations from the linear coupling code ALOHA [19]. This code takes into account realistic 3D antenna geometry and can cope with double electron density decay lengths (λ_n) in the scrape-off layer (SOL). The first density layer (λ_{n1} ~ mm) describes the private SOL between the side protections on the launcher, while the second density layer (λ_{n2} ~ cm) describes the main SOL. As can be seen in Fig. 3, good agreement between experiment and modelling is obtained.

Fig. 4 shows the comparison of the reflection coefficient obtained on the PAM launcher and on the Fully Active Multijunction (FAM) launchers previously used in Tore Supra, under similar experimental conditions. The figure clearly shows that the PAM has lower reflection coefficient than both FAM launchers, even though the plasma-launcher distance is larger and the electron density is lower.

4. Coupling during edge perturbations

Any additional heating system to be used in ITER must be able to maintain reliable power injection during ELMs. LHCD experiments were carried out with the PAM launcher in order to assess the reflection coefficient behaviour and power handling in the presence of edge perturbations. Since H-modes plasmas are not produced in Tore Supra, the edge perturbations were simulated by using supersonic molecular beam injection (SMBI). During each SMBI, the electron density in front of the launcher increases from ~2×10^{17}m^{-3} to ~10×10^{17}m^{-3} and the average reflection coefficient (RC) increases from 1.5% to 7% (Fig. 5).

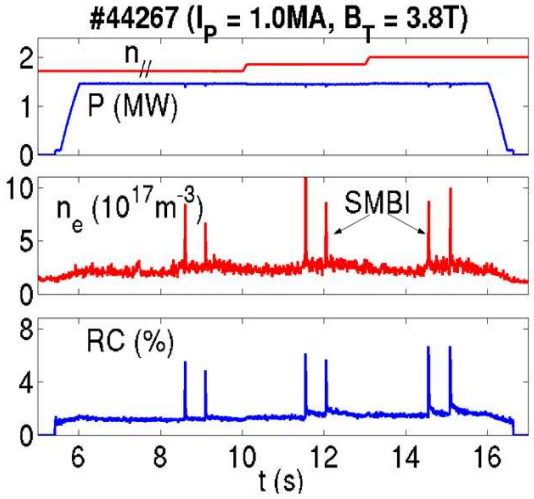

FIG. 5. Reflection coefficient behaviour during edge perturbations, produced by SMBI.

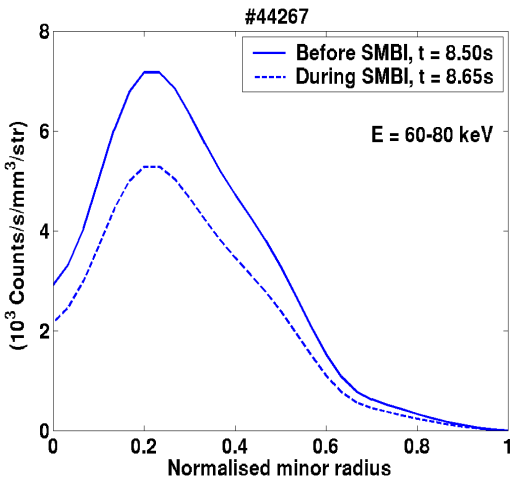

FIG. 6. Hard X-ray emission profile before and during SMBI. The hard X-ray profile, i.e. fast electron deposition profile, remains unchanged during the edge perturbation.

Detailed investigation of the RC behaviour during SMBI and ALOHA modelling show that the density decay length in the SOL increases during SMBI [20], which is also in agreement with edge measurements on Tore Supra. At least at intermediate power level (1.5MW, 13MW/m^2), the applied power remained constant during SMBI, indicating the possibility to couple during edge perturbations, such as ELMs. It should be noted that the present PAM launcher design for ITER [21] will give smaller variation in RC during an increase in density, making it a more ELM-resilient system.

In these experiments, the evolution of the hard X-ray emission (< 200keV) from the non-thermal electrons was studied during SMBI, as well as versus LHCD power, $n_{//}$ and electron density. During each SMBI, the hard X-ray signal falls, but the slow response of the hard X-ray emission suggests that it is due to the perturbation of the bulk density. As demonstrated in Fig. 6, the hard X-ray emission profile remains the same before and during, or immediately after SMBI, which indicates that the edge perturbation itself does not cause a redistribution of the fast electron profile [22].

5. High power operation

During the experimental campaign between autumn 2009 and spring 2010, the PAM has performed ~500 pulses on plasma. The maximum power and energy achieved on the PAM so far is 2.7MW during 78s flat-top, which results in an injected energy in a single discharge of 220MJ (Fig. 7). This record discharge was obtained after approximately 400 pulses on plasma, while the first goal of 2.7MW for shorter pulses (17s) was obtained after only 240 pulses on plasma. This power level corresponds to a power density of 25MW/m^2. At the present stage, the limitation is partly due to lack of generator power, partly due to conditioning of the waveguides. The launcher front face protection, based on the CuXIX-line emission and infrared thermography, detected very few arcs at the launcher mouth during all the experiments with the PAM. The infrared thermography shows that the apparent temperature of the waveguides and the side protections, which are actively cooled, remains below 270°C throughout #45472 (Fig. 8).

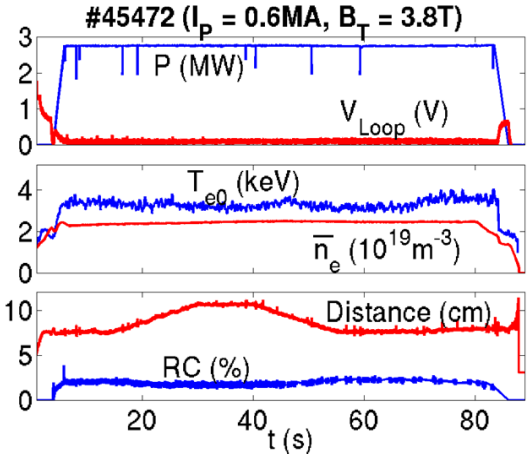

FIG. 7. Maximum power and energy achieved on the PAM launcher (2.7MW, 78s). Good coupling (RC < 2%) is maintained when the plasma-launcher distance is ramped to 10cm.

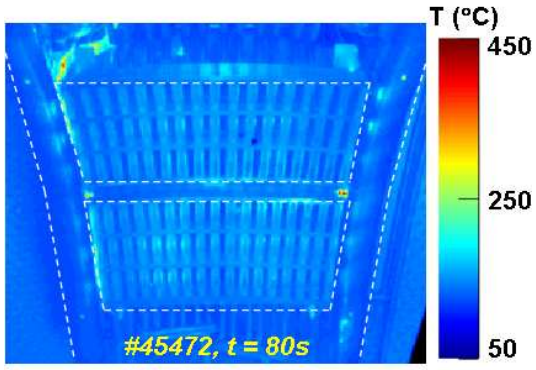

FIG. 8. Infrared image of the PAM launcher during the discharge with maximum injected energy on the PAM (#45472). The apparent temperature of the waveguides and side protections remain below 270°C.

Fig. 7 also demonstrates that high power can be coupled at large plasma-launcher distance. In #45472, the gap between the last closed flux surface (LCFS) and the launcher was increased to 10cm during the pulse. The reflection coefficient decreases slightly (from 2% to 1.5%) as the distance is increased. It has to be noted, however, that the density in front of the launcher was still above the cut-off density in these conditions, since the plasma scenario used was characterized by long SOL density decay length ($\lambda_n \sim 4$cm). This particular plasma scenario may therefore not be considered as representative of the plasma edge conditions that would be obtained during H-mode operation in ITER.

In the high power experiments, measurements with a retarding field analyzer [23] were made in order to obtain a detailed radial-poloidal mapping of the fast electron beam in front of the waveguide rows. This fast electron beam is caused by parasitic absorption in front of the launcher and known to be responsible for hot spots on plasma facing components. Preliminary results indicate that the electron beam current is less intense with the PAM launcher than with a FAM launcher under similar experimental conditions. This result remains however to be confirmed in experiments with the PAM and FAM launcher on the same plasma target.

6. Non-inductive current drive experiments

Full non-inductive pulses lasting up to 50s (Fig. 9) have been performed with the PAM launcher, using real-time control loops to maintain the plasma current constant by adjusting the LHCD power and to maintain the primary flux consumption at zero by acting on the central solenoid voltage. $P_{LHCD} = 2.2$MW was required to maintain $I_P = 0.51$MA and $V_{Loop} = 0$ at $\bar{n}_e = 1.45\times10^{19}$m^{-3}. The peak value of the parallel refractive index was $n_{//} = 1.72$, which corresponds to the optimum value, i.e. giving highest power directivity on the PAM. The value of the current drive efficiency (i.e. $\eta_{CD} = \bar{n}_e R_0 I_{CD} / P_{CD}$, where I_{CD} is the current driven by LHCD and P_{CD} is the coupled LHCD power) for the discharge in Fig. 9 was approximately 0.75×10^{19}m^{-2}A/W, taking into account a bootstrap current fraction of 10% (i.e. $I_{CD} = 0.9\times I_P$).

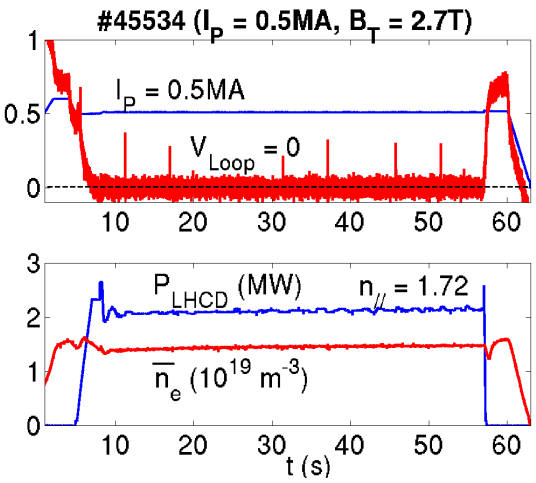

FIG. 9. Full non-inductive current drive sustained during 50s. The LHCD power is feedback controlled to maintain constant I_P, while V_{Loop} is maintained at zero by a feedback loop on the central solenoid voltage.

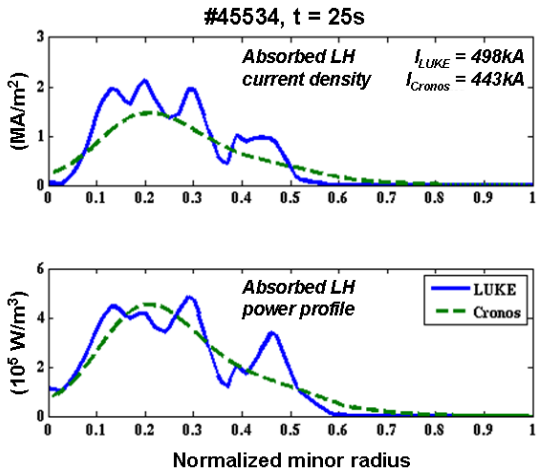

FIG. 10. Simulations of the LH driven current profile and absorbed LH power deposition profile for #45534, using CRONOS (dashed lines) and LUKE (solid lines).

Simulations of the LH driven current profile and LH power deposition profile using the CRONOS suite of codes [24] and the code CP3O/LUKE [25] are shown in Fig. 10. The CRONOS simulations uses the measured hard X-ray emission profile as input for the LH power deposition profile and reconstructs the plasma parameters, such as the flux consumption and internal inductance. The ray-tracing code CP3O and 3D relativistic Fokker-Planck code LUKE on the other hand uses the realistic LH wave spectrum computed by the ALOHA code as input. The ray-tracing calculation uses 36 rays to describe the launched $n_{//}$-spectrum: six poloidal launch locations (corresponding to six waveguide rows, see Fig. 2) and six $n_{//}$-values for each poloidal location (corresponding to the six largest peaks of the computed ALOHA $n_{//}$-spectrum). Good agreement between CRONOS and CP3O/LUKE simulations, both in terms of profile and in terms of driven LH current, is obtained.

In these full non-inductive discharges at low density, the current drive efficiency on the PAM launcher was found to decrease by < 10% when the density in front of the launcher was increased by a factor of two, i.e. from ~3×10^{17}m^{-3} to ~6×10^{17}m^{-3}. This is in agreement with the ALOHA code calculations, that predict that the power directivity of the $n_{//}$-spectrum drops from 68% to 62% when the density in front of the launcher increases from 3×10^{17}m^{-3} to 6×10^{17}m^{-3}. In this edge density range, the current drive efficiency with the PAM is found to be comparable to that obtained with the FAM launchers, when using the same peak value of the $n_{//}$-spectrum, as for example in the GJ-discharges [26].

Finally, experiments have also been conducted in Tore Supra with the aim to study the current drive efficiency of the lower hybrid waves at high electron density (up to $\bar{n}_e = 6\times10^{19}$m^{-3}), comparing gas fuelling and pellet fuelling. Although full non-inductive current drive could not be obtained, the evolution of the hard X-ray emission from the non-thermal electrons produced by LHCD was studied. The hard X-ray emission was found to decrease with volume average electron density, as ~$1/\bar{n}_e^{2.7}$, but with an even stronger decrease in gas fuelled discharges for $\bar{n}_e$ above 5×10^{19}m^{-3} [27].

7. Summary and outlook

The first experiments with the ITER-relevant Passive Active Multijunction (PAM) LHCD launcher in Tore Supra have shown extremely encouraging results in terms of reflection coefficient behaviour and power handling. Low reflected power level is obtained at low density in front of the launcher, i.e. close to the cut-off density. Very good agreement between the experimental reflection coefficient and the ALOHA code calculation is obtained. Long pulse operation at ITER-relevant power density has been demonstrated. So far, 25MW/m^2 (i.e. 2.7MW) has been obtained over pulse lengths up to 78s. High power (2.7MW) has been coupled at a plasma-launcher distance of 10cm with a power reflection coefficient lower than 2%. The current drive efficiency is comparable to that of the Fully Active Multijunction (FAM) launchers, at least in conditions with low density in front of the launcher. These results give good confidence for the design of an ITER LHCD launcher. The completion of the Tore Supra CIMES project, consisting of the upgrade of the LH generator plant to high power CW klystrons [16, 17], will allow to access regimes of zero loop voltage conditions at higher current and density than before and to perform long pulse operation up to 1000s.

Acknowledgments

The authors gratefully acknowledge the support of the Tore Supra Team, in particular of the CIMES project team. This work, supported by the European Communities under the contract of Association between EURATOM and CEA, was carried out within the framework of the European Fusion Development Agreement. The views and opinions expressed herein do not necessarily reflect those of the European Commission.

References

[1] PEYSSON, Y., in Radio Frequency Power in Plasmas, AIP Conf. Proc. **485** (1999) 183.
[2] TUCCILLO, A.A., et al., Plasma Phys. Control. Fusion **47** (2005) B363.
[3] YAMAMOTO, Y., et al., Phys. Rev. Lett. **45** (1980) 716.
[4] BERNABEI, S., et al., Phys. Rev. Lett. **49** (1982) 1255.
[5] BONOLI, P.T., et al., in Radio Frequency Power in Plasmas, AIP Conf. Proc. **694** (2003) 24.
[6] GORMEZANO, C., et al., Nucl. Fusion **47** (2007) S285.
[7] GARCIA, J., et al., Phys. Rev. Lett. **100** (2008) 255004.
[8] BIBET, PH., et al., Nucl. Fusion **35** (1995) 1213.
[9] BIBET, PH., et al., Fusion Eng. Des. **74** (2005) 419.
[10] HOANG, G.T., et al., Nucl. Fusion **49** (2009) 075001.
[11] MIRIZZI, F., et al., Fusion Eng. Des. **74** (2005) 237.
[12] PERICOLI RIDOLFINI, V., et al., Nucl. Fusion **45** (2005) 1085.
[13] BELO, J., BIBET, PH., et al., Fusion Eng. Des. **74** (2005) 283.
[14] GUILHEM, D., et al., in Radio Frequency Power in Plasmas, AIP Conf. Proc. **1187** (2009) 435.
[15] BEAUMONT, B., et al., Fusion Eng. Des. **56-57** (2001) 667.
[16] KAZARIAN, F., et al., Fusion Eng. Des. **84** (2009) 1006.
[17] DELPECH, L., et al., in Radio Frequency Power in Plasmas, AIP Conf. Proc. **1187** (2009) 431.
[18] EKEDAHL, A., et al., in Radio Frequency Power in Plasmas, AIP Conf. Proc. **1187** (2009) 407.

[19] HILLAIRET, J., et al., Fusion Eng. Des. **84** (2009) 953.
[20] PREYNAS, M., et al., *"Coupling characteristics of the ITER relevant lower hybrid antenna in Tore Supra: experiments and modeling"*. To be submitted for publication in Nucl. Fusion (2010).
[21] MILANESIO, D., et al., *"Benchmark of coupling codes (ALOHA, TOPLHA and GRILL3D) with ITER Lower Hybrid antenna"*, Paper P1-153 at 26th Symposium on Fusion Technology, Porto (2010). To be published in Fusion Eng. Des.
[22] SHARMA, P.K., et al., *"Hard X-ray measurements during LHCD experiments with passive active multijunction and fully active multijunction antennas in Tore Supra"*, Paper P5.184 at 37th EPS Conference on Plasma Physics, Dublin (2010).
[23] GUNN, J.P., et al., Journal Nuc. Mat. **390-391** (209) 904.
[24] ARTAUD, J.F., et al., Nucl. Fusion **50** (2010) 043001.
[25] PEYSSON, Y. and DECKER, J., in Radio Frequency Power in Plasmas, AIP Conf. Proc. **933** (2007) 293.
[26] VAN HOUTTE, D., et al., Nucl. Fusion **44** (2004) L11.
[27] GONICHE, M., et al., *"Lower hybrid current drive for the steady-state scenario"*, Accepted for publication in Plasma Phys. Control. Fusion (2010).